IEEE Access
Multidisciplinary | Rapid Review | Open Access Journal

Received 10 June 2024, accepted 27 June 2024, date of publication 2 July 2024, date of current version 12 July 2024.

Digital Object Identifier 10.1109/ACCESS.2024.3422240

RESEARCH ARTICLE

Design of Metamaterials for Absorbers Based on Variational Autoencoder

QI LI, JIANWEI WANG, TAO LEI, TIANYU XIANG, CHANCHAN QIN, AND MAOZE YANG
School of Big Data and Computer Science, Guizhou Normal University, Guiyang, Guizhou 550003, China

Corresponding author: Jianwei Wang (jianweiwang@gznu.edu.cn)

This work was supported by the Science and Technology Foundation of Guizhou Province of China under Grant ZK[2023]253.

ABSTRACT Metamaterials have experienced rapid development in recent years. Absorbers made of metamaterials play a crucial role in electromagnetic applications and other fields. The design of metamaterials is usually simulated using simulation software and optimized by traditional algorithms, which is time-consuming and difficult to optimize; deep learning, an emerging method, is gradually being used for both forward and inverse design of metamaterials, but few methods can simultaneously generate the geometric structure of metamaterials and meet the requirements of multiple physical spectra. This paper proposes an improved conditional variational autoencoder (conditional VAE), that is composed by an encoder and a decoder. The encoder generates a Gaussian distribution while acting as an inverse generated network to predict the corresponding geometric parameters. The decoder can generate absorption spectra that satisfy the requirements according to the conditions. By adding batch normalization and spectral normalization in network training, the convergence of the neural network is accelerated, and the stability of the network is increased. The results show that the encoder and decoder can accurately predict the geometric parameters and the absorption spectrum according to the conditions, proving the feasibility of the method. A structural sample of an absorber was processed and tested for verification. The method provides an effective way for the target design of absorbers and a new approach for the design of other electromagnetic metamaterials.

INDEX TERMS Absorber, deep learning, conditional VAE, inverse design.

I. INTRODUCTION

Metamaterials are artificially synthesized sub-wavelength scale composite materials that can achieve different operating properties of electromagnetic waves through periodic or non-periodic arrangements [1]. In recent years, metamaterials have shown good performance in regulating the amplitude, phase, polarization, and other aspects of electromagnetic waves, and have been widely used because of their good electromagnetic properties, such as negative refractive index [2], lenses [3], [4], perfect absorbers [5], [6], [7]and invisible cloaks [8]. Absorbers with high absorption rate, wide absorption frequency band [9], and flexible design have been studied for sensors [10], [11], electromagnetic interference shielding [12], heat emitters [13], solar energy collection [14].

The associate editor coordinating the review of this manuscript and approving it for publication was Guido Lombardi.

In general, researchers use electromagnetic simulation software to search for metamaterial structures or use some classic algorithms such as particle swarm optimization and topology algorithms to optimize metamaterials [15], [16], [17], [18], [19], [20], [21]. However, there is the problem of time-consuming, and the optimal solution is not always guaranteed in these processes.The development of deep learning has gained attention from researchers for its powerful learning and generalization capabilities [22], [23].Researchers use nonlinear models between input and output in deep learning to simulate the complex solving process between metamaterial geometric parameters and electromagnetic response [24], [25], which reduces workload and shortens time [26], [27].

Gu et al. proposed a forward and inverse design model for metamaterial absorbers consisting of a combination of primary and auxiliary networks(PPN and APN), which can achieve accuracy rates of 0.99 and 0.98 in forward prediction

© 2024 The Authors. This work is licensed under a Creative Commons Attribution-NonCommercial-NoDerivatives 4.0 License.
For more information, see https://creativecommons.org/licenses/by-nc-nd/4.0/

and inverse design, respectively. The method provides a basis for the design of absorbers [28]. Ma et al. designed an autoencoder network(CAN) and an inverse prediction network(IDN) model for the inverse design of an absorber. The model predicts low spectral errors and high accuracy of structural parameters, avoiding complex electromagnetic simulation processes [29]. Han et al. proposed an irregular absorber unit structure, which uses absorptivity and structural parameters as inputs and outputs for forward and inverse design, respectively. The error between the predicted and true values of the geometric parameters on the validation set can reach 0.0017, giving a pathway for the implementation of complex metamaterial structure design [30]. Hou et al. designed an inverse neural network model(FTNN,GNN and PNN) for customized absorbers using the absorption spectrum as an intermediate result [31]. The results show that the automatic generation time is short and accurate. Lin et al. used generative adversarial networks(GAN) to realize the one-to-many inverse design of absorbers under a given target, providing researchers with multiple choices [32]. The method offers a case for one-to-many design using deep learning. However, models combining multiple neural networks need to be trained multiple times, generative adversarial network models are difficult to train and have problems with mode collapse [33]. Therefore, it is necessary to design an enhanced neural network that is easy to train and capable of completing the inverse process for a given goal, while also providing multiple solutions to researchers.

In this paper, the use of an improved conditional VAE is proposed for the design of target absorbers. The conditional VAE [34] consists of an encoder and a decoder, the input of the encoder is the absorption spectrum and the target frequency bandwidth interval (range with the absorption rate of more than 90%), which is composed of a start frequency and an end frequency, the output is the distribution and geometric parameters of the latent space. The input of the decoder is the latent variables sampled from the latent space and the target frequency bandwidth. The output is multiple sets of absorption spectra that satisfy the target frequency. Moreover, weight initialization, batch normalization, and spectral normalization are added to accelerate the convergence of the network model. The method can generate absorber models that meet the requirements for researchers at a specified range, compared to the neural network spliced model, the model requires only one training cycle.We conduct performance studies on the absorber models used in neural networks at different polarization angles and incidence angles, respectively. A structural sample was made for experimental testing. In Section II, we describe the material model in Part A, the specific details of the proposed network structure in Part B, and the training process of the network model in Part C. In Section III, we obtain the results of the network model and analyze and discuss the results. In Section IV, we conclude the paper.

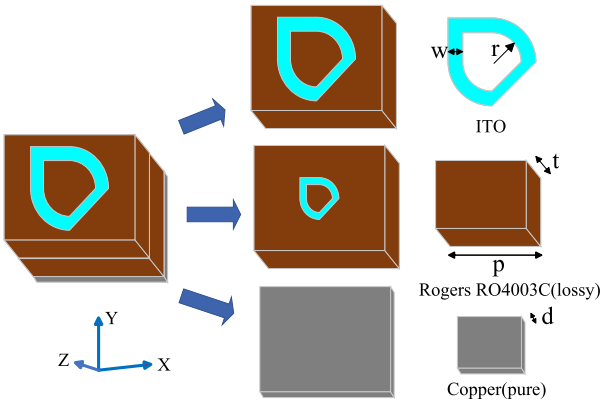

FIGURE 1. Schematic diagram of the proposed absorber model. The absorber model consists of two layers of ITO-resistive film alternating with two layers of Rogers RO4003C. A bottom layer of copper is present.

II. MATERIAL MODELS AND METHODS

A. ABSORBER STRUCTURE

To verify the effectiveness of the proposed deep learning method on metamaterial models, this paper implements the modeling of an absorber model. Fig.1 shows a schematic diagram of the proposed absorber model, the absorber model consists of five layers, the upper four layers are composed of two layers of ITO resistive film alternating with two layers of Rogers RO4003C (lossy) dielectric [35], [36], the bottom metal reflective backboard uses pure copper. The dielectric constant and loss tangent angle of Rogers RO4003C (lossy) are 3.5 and 0.0027, respectively. The unit period p is fixed at 6 mm, and the thickness d of the bottom metal is 0.035 mm. The pattern shape of the resistive film is made up of an L-shape, a diagonal stripe, and a 90° fan ring. The design parameters of the absorber model are the distance $r1$ from the center of the first layer of resistive film pattern to the fan ring, the width of the fan ring $w1$, the surface impedance $R1$ of the resistive film, the thickness of the second layer dielectric $t1$, the distance $r2$ from the center of the third layer resistive film pattern to the fan ring, the width of the fan ring $w2$, the surface impedance $R2$ of the resistive film, the thickness of the fourth layer dielectric $t2$. Due to the physical size limitation of the material unit period, the shape of the resistive film pattern should fulfill several conditions, $r1 + w1 < p/2, r2 + w2 < p/2$.

The above proposed absorber model is modeled using the commercial software CST Microwave Studio. Using a frequency domain solver based on the finite element method and setting the simulation frequency interval to 2GHz∼22GHz. Periodic boundary conditions are used for the x-axis and y-axis, and open (add space) is used for the z-axis. Scanning the above eight geometric parameters and sampling at equal intervals within the parameter physical size constraints, as shown in Table 1. To obtain the dataset containing geometric parameters and absorption spectrum relationships required for deep model training, the

TABLE 1. Range of geometric parameters of the absorber.

Parameters	Minimum	Maximum	sample size
$r1(mm)$	0.2	1.5	2070
$w1(mm)$	0.4	1.4	2000
$R1(\Omega/sq)$	25	85	600
$t1(mm)$	1.2	4.8	2020
$r2(mm)$	0.2	1.5	2070
$w2(mm)$	0.2	1.4	2041
$R2(\Omega/sq)$	25	80	550
$t2(mm)$	1	5	2050

corresponding S_{11} parameters of the model are obtained in the simulation process, by applying (1), the corresponding absorption rate can be calculated.

$$A = 1 - |S_{11}|^2 \tag{1}$$

where A is the absorbance, S_{11} is the reflection coefficient.

B. NETWORK MODEL

Conditional VAE network consists of two parts: an encoder and a decoder. Among them, the input data of the encoder is the absorption spectrum and condition, which is the corresponding frequency bandwidth interval absorption of more than 90%. Previously, the encoder was only used to output a latent space distribution [37],the decoder is mainly used in the data generation process,and function of the encoder is very single, so, for this generative model of the variational autoencoder, which is an underutilization of encoder network resources. To make better use of the encoder, a new architecture of the encoder network is proposed here, which uses the encoder as an inverse designed network to generate geometric parameters while generating latent space distributions. The input data to the decoder are the conditions and the latent space variables obtained by sampling from the latent space distribution, and the output data is the reconstructed absorption spectrum. The process of the model is shown in Fig.2.

The encoder consists of one-dimensional convolutional layers and fully connected (FC) layers, the one-dimensional convolutional layer is used to extract features from the absorption spectrum, and the size of the convolutional kernel used in the convolutional layer is 3, at the same time, the structure of residual blocks is used in the convolutional layer [38]. On the one hand, residual blocks can effectively alleviate the problems of gradient vanishing and gradient explosion, making encoder training much easier. On the other hand, residual blocks can learn more complex and detailed feature representations to improve the performance of inverse design.The dimensions of the input and output data of the first convolutional layer and residual block are different from those of the second one. The fully connected layer is used for dimensional transformation and feature mapping after the convolutional layer. Besides, using batch normalization after one-dimensional convolutional or fully connected layers to accelerate network convergence. To ensure stable training of the encoder, both the convolutional layer and the fully connected layer are initialized. The specific architecture of the encoder network is shown in Fig.3.

TABLE 2. Details of the decoder, FC layer is a fully connected layer.

Layer	Dimensions	Activation Function
Input	20+2	\
FC layer1	64	Relu
FC layer2	128	Relu
FC layer3	128	Relu
Output	125×2	\

TABLE 3. Results of network models with different frequency points selected from the absorption spectrum. The error value is the reconstruction error.

	Training time(minutes)	Error value	Model size(MB)
125 points	38	0.002	3.8
251 points	54.7	0.016	10.5
501 points	70.5	0.094	20.7

TABLE 4. Comparison of results before and after using residual blocks.

Models	Train loss	Time(minutes)
FC	0.94	57
Redidual block	0.12	38

The decoder is composed of four fully connected layers. The inputs are condition and latent variables, and after fully connected layers nonlinear factors are introduced using an activation function Relu, and the output is the absorption spectrum curve. However, since the process of sampling is a non-differentiable operation, the gradient of the neural network breaks down here and back propagation is not possible. Therefore, the reparameterization technique is used, sampling from a standard normal distribution to obtain a 20 dimensional vector, multiplying it with the standard deviation of the latent space distribution generated by the encoder to obtain the result, and then adding it to the mean to generate the latent variable. This process only involves linear operations, which is differentiable.The decoder aims to generate absorption spectra that meet the target conditions according to the requirements.The detailed structural information of the decoder is shown in Table2.

C. TRAINING MODELS

To collect the dataset needed for model training and obtain the relationship between the absorption spectrum and geometric parameters.Using Python combined with electromagnetic simulation software CST, automatically changes the geometric parameters for simulation and saves the corresponding data. To facilitate the training of the neural network and maintain the feature of the data, as can be seen from the comparison of the different frequency points in Table 3, the absorption spectrum is simplified by selecting 125 points in the absorption spectrum at equal intervals. A total of 13401 corresponding data are collected, of which 10720(80%) are used as the training dataset and 2681(20%) are used as the testing dataset. The encoder and decoder are

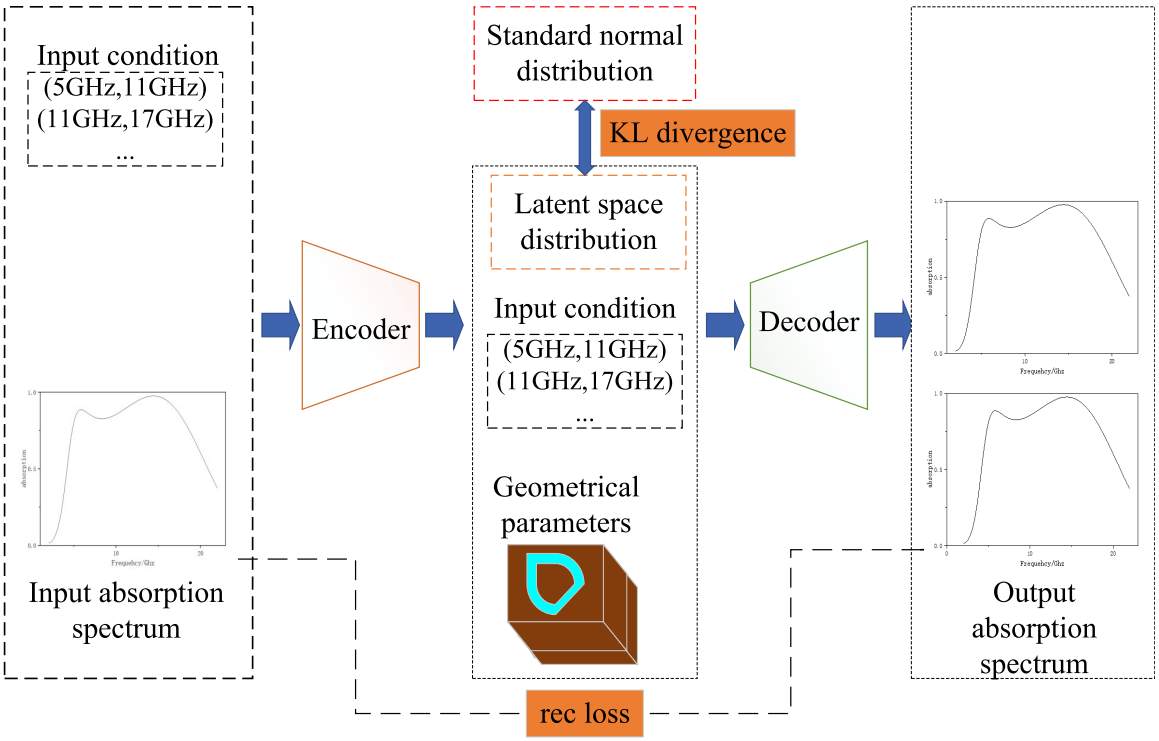

FIGURE 2. Flowchart of the improved conditional VAE. The encoder takes the target frequency interval, i.e., the input conditions [start frequency,end frequency] and the absorption spectrum as input and outputs the latent space distribution and geometric parameters. The decoder reconstructs the absorption spectrum from the target frequency interval and the latent variables sampled from the latent space.

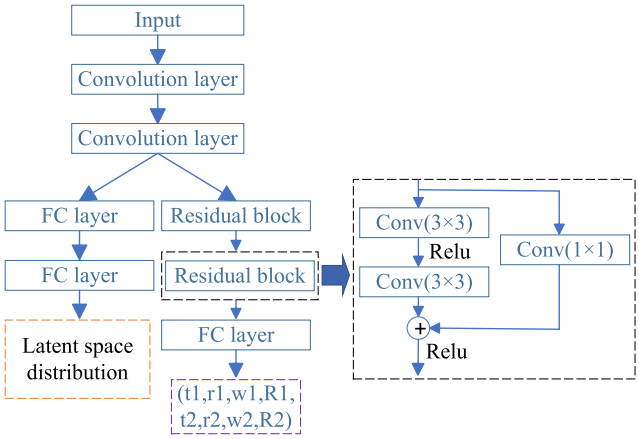

FIGURE 3. Schematic diagram of an encoder network composed of one-dimensional convolutional layers, residual blocks, and fully connected layers. Input is the absorption spectrum. Outputs are latent space distribution and geometric parameters.

trained using Adam optimizer. Relu is used as the activation function between neuron layers, the batch size is set to 32, the learning rate is set to 0.0005, and the epoch is set to 300. The model is trained on a 12th Gen Intel(R) Core (TM) i5-12500 laptop.

According to the theory of the conditional VAE, it is known that the loss function of the conditional VAE model has two parts as shown in the (2),

$$\mathcal{L}(\theta, \phi; x, z) = \mathbb{E}_{q_\phi(z|x)}[\log p_\theta(x|z)] - D_{KL}(q_\phi(z|x)\|p(z)) \tag{2}$$

θ and ϕ represent the network parameters for the decoder and encoder, respectively, p_θ is the likelihood under the model, q_ϕ is the approximate posterior, x is the input spectral data, and z is the latent variable.One part is the reconstruction error $\mathbb{E}_{q_\phi(z|x)}$ between the absorption spectrum of the encoder input and the spectrum generated by the decoder, which is measured using the mean square error (MSE) as shown in the (3),

$$Loss_{recon} = \frac{1}{n}\sum_{i=1}^{n}(A_{rec} - A_{real})^2 \tag{3}$$

where n represents the number of samples, A_{rec} represents the reconstructed absorption spectrum, A_{real} represents the real absorption spectrum. Our goal is to minimize this error, the smaller its value, the more accurate the reconstructed absorption spectrum is, and the error value is a measure of the decoder's performance. The other part is the distance D_{KL} between the Gaussian distribution of the latent space generated by the encoder and the standard normal distribution. Generally, Kullback-Leibler divergence (KL divergence) is used to measure the distance between the two distributions,

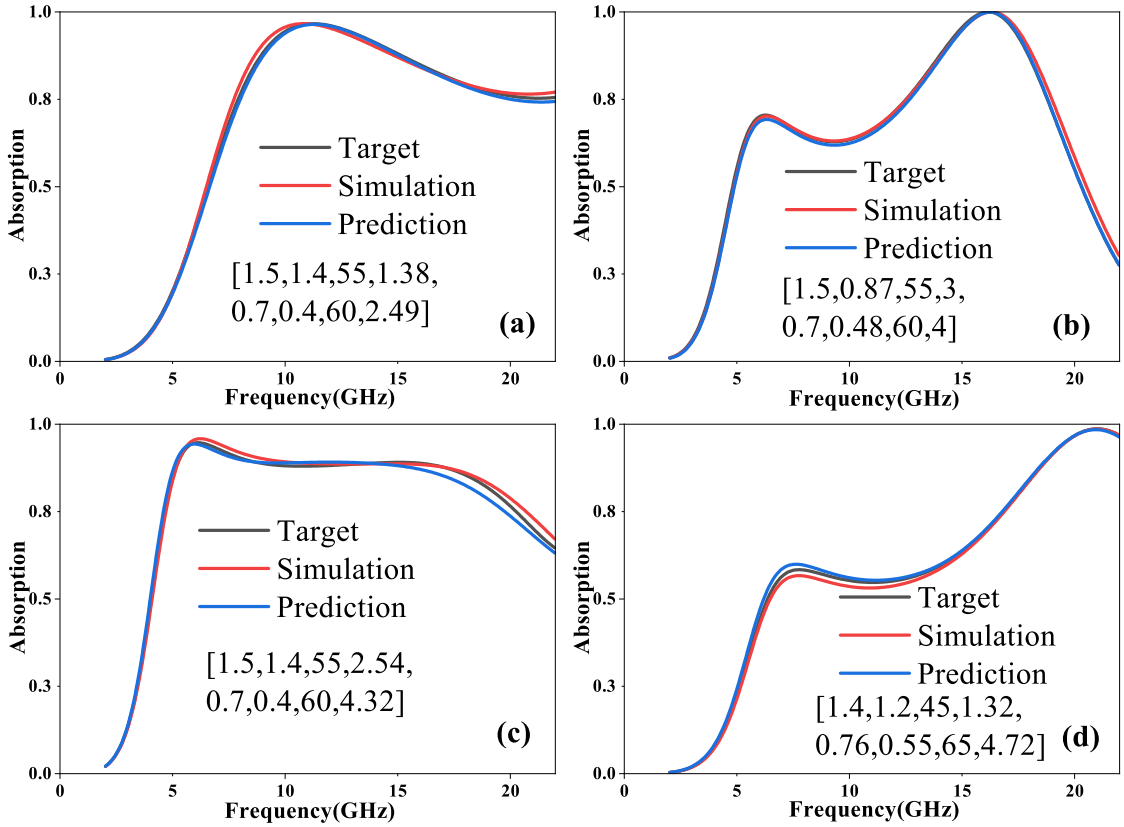

FIGURE 4. (a), (b), (c), (d) are four randomly selected samples from the test set to test the encoder network's inverse prediction ability. The black curve represents the target absorption spectrum, and the red curve represents the simulated absorption spectrum obtained based on the geometric parameters predicted by the network. The blue curve represents the predicted absorption spectrum based on the network. The geometric parameters [$r1$, $w1$, $R1$, $t1$, $r2$, $w2$, $R2$, $t2$] corresponding to the curves are provided in each insets.

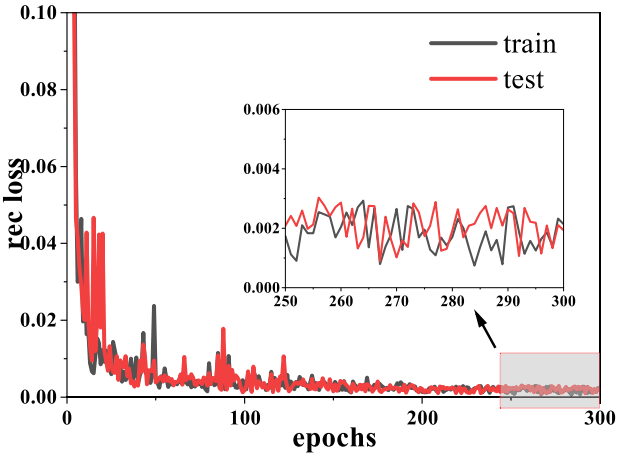

FIGURE 5. Reconstruct the loss curve. Values converge to 0.002.

as shown in the (4),

$$Loss_{kld} = KL\big(N(\mu_x, \sigma_x), N(0, 1)\big) \tag{4}$$

where μ_x represents the mean value obtained from the latent space, and σ_x represents the standard deviation obtained from the latent space, the closer the distance between distributions, the smaller the KL divergence value. Additionally, we also use the encoder as an inverse generated network, then there is an error between the predicted geometric parameters and the true geometric parameters, again using the MSE as a measure of the error between the geometric parameters, as shown in the (5),

$$Loss_{geom} = \frac{1}{n}\sum_{i=1}^{n}(P_{pre} - P_{real})^2 \tag{5}$$

where P_{pre} represents the predicted structural parameter, P_{real} represents the real structural parameters.Since the neural network used is based on a gradient descent algorithm, it is a minimization total loss function,as shown in the (6),

$$Loss_{total} = Loss_{recon} + Loss_{kld} + Loss_{geom} \tag{6}$$

In the process of model training, as the number of iterations increases, the value of the loss function gradually decreases. When the value of the loss function stops decreasing and stabilizes, the network model converges, which means that training can end. At this time, the parameters in the variational autoencoder are no longer updated, then the training is complete.

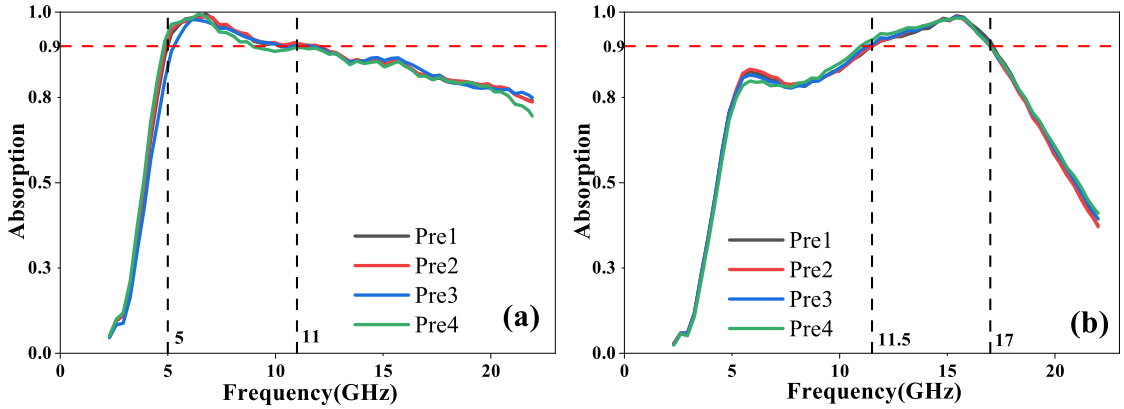

FIGURE 6. Decoder network prediction results. (a) Prediction results for target frequency interval at 5-11Ghz. (b) Prediction results for target frequency interval at 11.5-17Ghz.

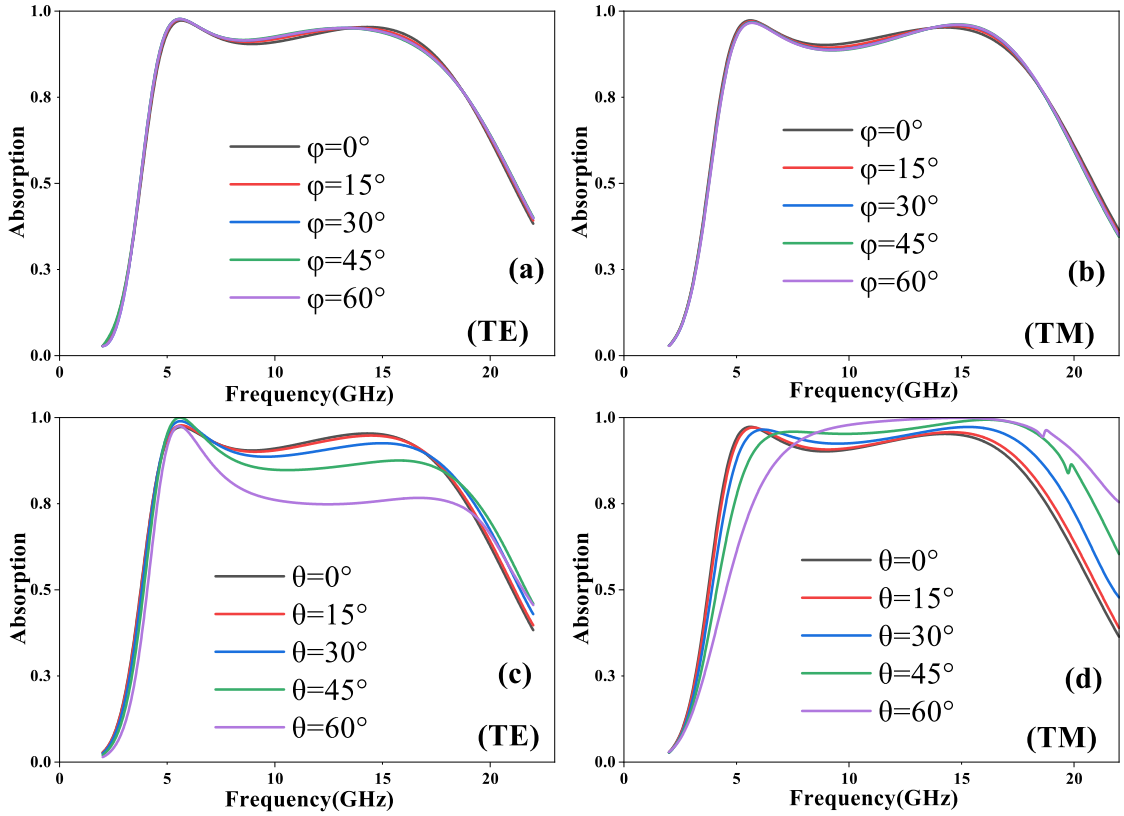

FIGURE 7. Absorption spectra of the absorber at different polarization angles in TE mode (a), different polarization angles in TM mode (b), different angles of incidence in TE mode (c) and different angles of incidence in TM mode (d), respectively.

III. RESULTS AND DISCUSSION

After the training of the conditional VAE is completed, it is necessary to evaluate the predictive effect and performance of the network model. Firstly, the encoder needs to be able to learn the features of the absorption spectrum and encode them into the distribution of the latent space. After stabilizing the model's parameters, the KL divergence value between the generated latent space distribution and the standard normal distribution is 0.036, indicating that the encoder is effective for feature compression of the absorption spectrum. It ensures that the latent space has good properties for data generation, which facilitates the decoding of features from the random samples from the latent space.

Secondly, the encoder is also regarded as a network for inverse design, and the encoder is tested during the inverse design process using the test set data and the MSE loss value on the model is 0.12. From Table4, it can be seen that the inclusion of the residual network reduces both the training error value and the training time, demonstrating that the addition of the residual block is effective. Meanwhile,

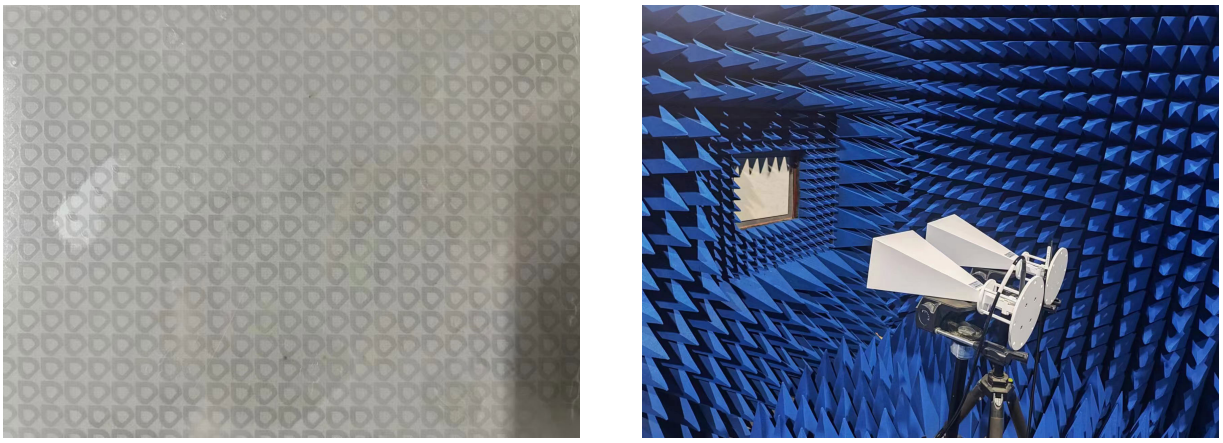

(a) (b)

FIGURE 8. Absorber sample(a) and test environment(b).

four sets of data are randomly selected, and the geometrical parameters predicted by the encoder are simulated to obtain the absorption spectrum using the electromagnetic simulation software CST, and the simulated results are compared with the target spectrum, as shown in the Fig.4. Obviously, the curve of the simulation results is basically consistent with the target absorption spectrum curve, the accurate prediction results of four sets of spectral curves in different frequency bands indicate that the encoder can be trained for inverse design. By using the improved encoder, it can perform a good inverse design while compressing the absorption spectrum features. There is no need to build an additional network model to complete the inverse design, saving resources, which is one of the advantages of the proposed network.

Then, a decoder network is used to perform the design of a one-to-many absorption spectrum. During the training process, the decoder network is used to reconstruct the absorption spectrum. After the training is completed, the decoder is tested using the test set data to obtain the reconstruction error of the decoder, as shown in the Fig.5, it can be seen that at 300 epochs, the reconstruction error of the decoder tends to a stable value of 0.002, indicating that the decoder can accurately reconstruct the absorption spectrum. Within the simulation frequency band, two target demands are selected and sampled from the latent space, only using the decoder network to design the absorption spectrum for the specified absorption frequency band, as shown in the Fig.6. From the results, the absorption rate of the absorption curve can reach over 90% within the target range[5,11]GHz and [11.5, 17]GHz, and analysis of the generated absorption spectrum reveals that the decoder can generate some curves outside the dataset, some of the absorption spectra generated are similar. For the same target condition, different solutions can be obtained. Overall, the generated absorption curves meet the condition, indicating that the decoder can learn features from latent space and has a generalization ability to achieve specific spectrum design.Comparing the model proposed in this paper with some models in existing references has excellent advantages, as shown in Table5.

TABLE 5. Comparison results between our model and other models. P is the material unit period and BW is the frequency bandwidth interval (range with the absorption rate of more than 90%).

Refs.	Stability	P(mm)	BW(GHz)	Design scheme
[28]	good	nanoscale	\	PPN+APN
[29]	general	16	3.6-18	CAN+IDN
[31]	weak	12	7-20	FTNN+GNN+PNN
[32]	general	12	7-24	GAN
This work	good	6	4-22	CVAE

We observed the absorption performance of the designed absorber model at different polarization and incidence angles. A set of geometrical parameters of the model is selected, simulated in the electromagnetic simulation software CST, and calculated using the template function to obtain the absorptivity. Five different polarization angles and incidence angles equally spaced within [0 °,60 °] are set for parameter scanning respectively, and the results are shown in the Fig.7. Observing that as the polarization angle gradually increases, there is almost no change in the absorption curve of the TE and TM modes, indicating that the designed structure is polarization insensitive. Meanwhile, it can be observed that the absorption rates between 5GHz and 17GHz are all more than 90%, achieving broadband absorption of the absorber, then the designed absorber model can provide a reference for the broadband absorption. From the Fig.7, it is found that as the incident angle increases, the absorption curve gradually decreases in TE mode and shifts in TM mode, which indicates that the structure is incident sensitive. After 45 °, the absorption drops to less than 80%. To maintain the high absorption characteristics of the absorber, the incidence angle should be less than 45 ° in applications.

Finally, we made a sample with a total size of $240mm \times 240mm$, containing 40×40 periodic structures. Since the simulation band of the designed structure is in the 2-22GHz

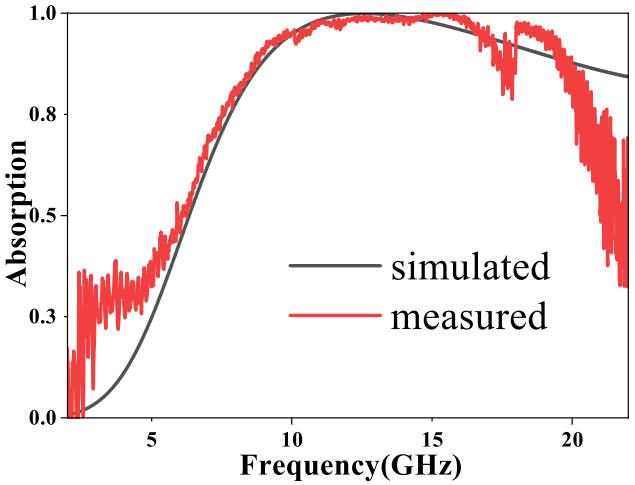

FIGURE 9. Comparison figure of simulation and test. The black curve is the simulation result, and the red curve is the test result.

range, the horn with operating bands in the range of 1-18 GHz and 18-26.5 GHz is used for separate measurements in the microwave darkroom. The type of vector network analyzer used was the Ceyear 3672c. Sample and the testing environment are shown in the Fig.8. As shown in the Fig.9, the results of the predicted structural simulation are consistent with the measured results, indicating that the method is effective for absorber design.

IV. CONCLUSION

In summary, this paper proposes a method for inverse designing the conditional VAE of an absorber based on the target absorption frequency.The conditional VAE consists of two parts: an encoder and a decoder. The method improves the encoder, allowing it to generate a Gaussian distribution latent space while also serving as an inverse generated network to predict corresponding geometric parameters. Applying batch normalization and residual blocks to the encoder increases the speed and accuracy of network training. The results show that the geometric parameter error value predicted by the encoder is as low as 0.12 and the predicted spectrum is consistent with the simulation spectrum results. The decoder can realize the design of one-to-many absorption spectra according to the target requirements,and the results show that the implemented spectrum curve is different. Due to the generalization ability of conditional VAE, there have also been some schemes that satisfy the conditions and are not in the dataset. Furthermore, we have simulated the designed absorber model for multiple incidence angles and multiple polarization angles, respectively. And the designed absorber performs well. The actual experimental results show that the structure predicted by the neural network is relatively accurate. Compared with previous neural network models, the method is simple to train and can simultaneously generate geometric parameters and absorption spectra that meet the target requirements. Hence, we believe that this easy-to-train and highly accurate neural network method can provide convenience for researchers to inverse design absorber structures as needed, and even transfer the method to other electromagnetic metamaterial models for the required design.

REFERENCES

[1] T. J. Cui, S. Liu, and L. Zhang, "Information metamaterials and metasurfaces," *J. Mater. Chem. C*, vol. 5, no. 15, pp. 3644–3668, 2017.
[2] S. B. Glybovski, S. A. Tretyakov, P. A. Belov, Y. S. Kivshar, and C. R. Simovski, "Metasurfaces: From microwaves to visible," *Phys. Rep.*, vol. 634, pp. 1–72, May 2016.
[3] T. Roy, S. Zhang, I. W. Jung, M. Troccoli, F. Capasso, and D. Lopez, "Dynamic metasurface lens based on MEMS technology," *APL Photon.*, vol. 3, no. 2, pp. 1–12, Feb. 2018.
[4] M. Khorasaninejad, W. T. Chen, R. C. Devlin, J. Oh, A. Y. Zhu, and F. Capasso, "Metalenses at visible wavelengths: Diffraction-limited focusing and subwavelength resolution imaging," *Science*, vol. 352, no. 6290, pp. 1190–1194, Jun. 2016.
[5] J. Li, Y.-H. Wang, R.-C. Jin, J.-Q. Li, and Z.-G. Dong, "Toroidal-dipole induced plasmonic perfect absorber," *J. Phys. D, Appl. Phys.*, vol. 50, no. 48, Dec. 2017, Art. no. 485301.
[6] Z. Liu, G. Liu, X. Liu, Y. Wang, and G. Fu, "Titanium resonators based ultra-broadband perfect light absorber," *Opt. Mater.*, vol. 83, pp. 118–123, Sep. 2018.
[7] Y. Yao, J. Zhou, Z. Liu, X. Liu, G. Fu, and G. Liu, "Refractory materials and plasmonics based perfect absorbers," *Nanotechnology*, vol. 32, no. 13, Mar. 2021, Art. no. 132002.
[8] M. Fazeli, S. H. Sedighy, and H. R. Hassani, "Arbitrary shaped homogeneous invisible ground cloak," *Appl. Comput. Electromagn. Soc. J.*, vol. 31, no. 11, pp. 1–23, 2016.
[9] X. Li, X.-M. Chen, S.-B. Wu, and Y. Wang, "Design of ultra-broadband metamaterial absorber from visible to infrared region," *Plasmonics*, pp. 1–9, 2024.
[10] R. Yahiaoui, S. Tan, L. Cong, R. Singh, F. Yan, and W. Zhang, "Multispectral terahertz sensing with highly flexible ultrathin metamaterial absorber," *J. Appl. Phys.*, vol. 118, no. 8, pp. 68–72, Aug. 2015.
[11] L. Pan, Y. Xie, H. Yang, M. Li, X. Bao, J. Shang, and R.-W. Li, "Flexible magnetic sensors," *Sensors*, vol. 23, no. 8, p. 4083, Apr. 2023.
[12] J. Liu, M.-Y. Yu, Z.-Z. Yu, and V. Nicolosi, "Design and advanced manufacturing of electromagnetic interference shielding materials," *Mater. Today*, vol. 66, pp. 245–272, Jun. 2023.
[13] H. Yuan, H. Zhang, K. Huang, Y. Cheng, K. Wang, S. Cheng, W. Li, J. Jiang, J. Li, C. Tu, X. Wang, Y. Qi, and Z. Liu, "Dual-emitter graphene glass fiber fabric for radiant heating," *ACS Nano*, vol. 16, no. 2, pp. 2577–2584, Feb. 2022.
[14] H. Wang, V. Prasad Sivan, A. Mitchell, G. Rosengarten, P. Phelan, and L. Wang, "Highly efficient selective metamaterial absorber for high-temperature solar thermal energy harvesting," *Sol. Energy Mater. Sol. Cells*, vol. 137, pp. 235–242, Jun. 2015.
[15] H. Yu, M. Jiang, Y. Guo, T. Turiv, W. Lu, V. Ray, O. D. Lavrentovich, and Q. Wei, "Plasmonic metasurfaces with high UV–Vis transmittance for photopatterning of designer molecular orientations," *Adv. Opt. Mater.*, vol. 7, no. 11, Jun. 2019, Art. no. 1900117.
[16] Y. Hua, K. Chen, Y. Fu, and X. Zhang, "The direction switching control of electromagnetic waves based on all-dielectric metamaterials," *Appl. Comput. Electromagn. Soc. J.*, vol. 34, no. 7, pp. 1–17, 2019.
[17] K. Liang, J. He, Z. Jia, and X. Zhang, "Topology optimization of magnetorheological smart materials included PnCs for tunable wide bandgap design," *Acta Mechanica Sinica*, vol. 38, no. 3, Mar. 2022, Art. no. 421525.
[18] D. Chen, M. Skouras, B. Zhu, and W. Matusik, "Computational discovery of extremal microstructure families," *Sci. Adv.*, vol. 4, no. 1, Jan. 2018, Art. no. eaao7005.
[19] S. D. Campbell, D. Sell, R. P. Jenkins, E. B. Whiting, J. A. Fan, and D. H. Werner, "Review of numerical optimization techniques for meta-device design," *Opt. Mater. Exp.*, vol. 9, no. 4, pp. 1842–1863, Apr. 2019.
[20] Y. Zhou, X. Cao, J. Gao, S. Li, and X. Liu, "RCS reduction for grazing incidence based on coding metasurface," *Electron. Lett.*, vol. 53, no. 20, pp. 1381–1383, Sep. 2017.

[21] C. Wang, X.-F. Li, S.-J. Zhang, and R.-Z. Wang, "Design of broadband gradient resistive film metamaterial absorber based on genetic algorithm," *Acta Phys. Sinica*, vol. 73, no. 7, 2024, Art. no. 074101.
[22] W. G. Hatcher and W. Yu, "A survey of deep learning: Platforms, applications and emerging research trends," *IEEE Access*, vol. 6, pp. 24411–24432, 2018.
[23] T. Qiu, X. Shi, J. Wang, Y. Li, S. Qu, Q. Cheng, T. Cui, and S. Sui, "Deep learning: A rapid and efficient route to automatic metasurface design," *Adv. Sci.*, vol. 6, no. 12, Jun. 2019, Art. no. 1900128.
[24] Z. Liu, D. Zhu, S. P. Rodrigues, K.-T. Lee, and W. Cai, "Generative model for the inverse design of metasurfaces," *Nano Lett.*, vol. 18, no. 10, pp. 6570–6576, Oct. 2018.
[25] F. Liu, W. Zhang, Y. Sun, J. Liu, J. Miao, F. He, and X. Wu, "Secure deep learning for intelligent terahertz metamaterial identification," *Sensors*, vol. 20, no. 19, p. 5673, Oct. 2020.
[26] S. Wang, Q. Ma, Z. Wei, R. Wu, W. Ding, and J. Guo, "Deep-learning-assisted design of multi-degree-of-freedom metamaterial absorber," *Phys. Scripta*, vol. 99, no. 5, May 2024, Art. no. 055531.
[27] S. Wang, Q. Ma, Y. Chen, W. Ding, and J. Guo, "Inverse design of polymorphic reconfigurable metamaterial absorbers based on a dual-input neural network," *J. Phys. D, Appl. Phys.*, vol. 57, no. 27, Jul. 2024, Art. no. 275106.
[28] L. Gu, H. Liu, Z. Wei, R. Wu, and J. Guo, "Optimized design of plasma metamaterial absorber based on machine learning," *Photonics*, vol. 10, no. 8, p. 874, 2023.
[29] J. Ma, Y. Huang, M. Pu, D. Xu, J. Luo, Y. Guo, and X. Luo, "Inverse design of broadband metasurface absorber based on convolutional autoencoder network and inverse design network," *J. Phys. D, Appl. Phys.*, vol. 53, no. 46, Nov. 2020, Art. no. 464002.
[30] C. Han, B. Zhang, H. Wang, and J. Ding, "Metamaterial perfect absorber with morphology-engineered meta-atoms using deep learning," *Opt. Exp.*, vol. 29, no. 13, p. 19955, 2021.
[31] J. Hou, H. Lin, W. Xu, Y. Tian, Y. Wang, X. Shi, F. Deng, and L. Chen, "Customized inverse design of metamaterial absorber based on target-driven deep learning method," *IEEE Access*, vol. 8, pp. 211849–211859, 2020.
[32] H. Lin, Y. Tian, J. Hou, W. Xu, X. Shi, and R. Tang, "Fussy inverse design of metamaterial absorbers assisted by a generative adversarial network," *Frontiers Mater.*, vol. 9, Jul. 2022, Art. no. 926094.
[33] N. Kodali, J. Abernethy, J. Hays, and Z. Kira, "On convergence and stability of GANs," 2017, *arXiv:1705.07215*.
[34] A. Mishra, S. K. Reddy, A. Mittal, and H. A. Murthy, "A generative model for zero shot learning using conditional variational autoencoders," in *Proc. IEEE/CVF Conf. Comput. Vis. Pattern Recognit. Workshops (CVPRW)*, Jun. 2018, pp. 2269–22698.
[35] S. T. Imeci, B. Tütüncü, and L. Herceg, "Performance-enhanced S-shaped slotted patch antenna for X band/Ku band applications," *Wireless Pers. Commun.*, vol. 129, no. 2, pp. 1069–1082, Mar. 2023.
[36] X. Lei, Y. Li, S. Huo, Z. Sun, H. Yu, L. Fang, S. Xu, B. Li, M. Wang, and E. Li, "Design and analysis of a novel compact metamaterial absorber based on double-layer ITO resistive film for improving signal integrity," *IEEE Access*, vol. 10, pp. 24067–24079, 2022.
[37] D. P. Kingma and M. Welling, "Auto-encoding variational Bayes," 2013, *arXiv :1312.6114*.
[38] K. He, X. Zhang, S. Ren, and J. Sun, "Deep residual learning for image recognition," *Proc. CVPR*, vol. 16, pp. 770–778, Sep. 2016.

QI LI received the bachelor's degree in engineering management from Liaoning Petrochemical University, in 2021. He is currently pursuing the master's degree in computer science and technology with Guizhou Normal University. His current research interest includes deep learning in the design and optimization of metamaterials.

JIANWEI WANG received the bachelor's degree in electrical engineering and automation from Harbin Institute of Technology, in 2009, and the Ph.D. degree in engineering from Sungkyunkwan University, South Korea, in 2015. He is currently the Director of the Department of Information Engineering, School of Big Data and Computer Science, Guizhou Normal University. His research interests include microwave technology, electromagnetic materials, and machine learning.

TAO LEI received the Ph.D. degree in electronic science and technology from Guizhou University, in 2014. He was a Postdoctoral Researcher with the State Key Laboratory of Millimeter Wave, Southeast University. He is currently an Associate Professor with Guizhou Normal University. He is mainly engaged in research on radio frequency technology and electromagnetic metasurfaces in wireless communication systems.

TIANYU XIANG received the Ph.D. degree in radio physics from Central China Normal University, in 2020. She is mainly engaged in research on radio frequency technology and electromagnetic metamaterials in wireless communication systems.

CHANCHAN QIN received the Ph.D. degree from Central China Normal University. She mainly engages in theoretical and applied research in fields, such as computer vision, artificial intelligence, and filter design.

MAOZE YANG received the bachelor's degree in materials science and engineering from Guizhou Education University, in 2023. He is currently pursuing the master's degree in electronic information and communication engineering with Guizhou Normal University. His current research interests include radio frequency identification and graphene as a gas-sensitive material.